

# NUMERICAL MODELING OF THE COMBUSTION SYNTHESIS OF TiAl/Al<sub>2</sub>O<sub>3</sub> COMPOSITE VIA MICROWAVE HEATING

S. Ghafurian<sup>1</sup>, S. H. Seyedein<sup>1</sup>, M. R. Aboutalebi<sup>1,\*</sup> and M. Reza Afshar<sup>2</sup>

\* mrezab@iust.ac.ir

Received: March 2011

Accepted: July 2011

<sup>1</sup> Centre of Excellence for Advanced Materials and Processing (CEAMP), School of Metallurgy & Materials Eng., Iran University of Science and Technology, Tehran, Iran.

<sup>2</sup> Department of Material Engineering, Science and Research Branch, Islamic Azad University, Tehran, Iran.

**Abstract:** Microwave processing is one of the novel methods for combustion synthesis of intermetallic compounds and composites. This method brings about a lot of opportunities for processing of uniquely characterized materials. In this study, the combustion synthesis of TiAl/Al<sub>2</sub>O<sub>3</sub> composite via microwave heating has been investigated by the development of a heat transfer model including a microwave heating source term. The model was tested and verified by experiments available in the literature. Parametric studies were carried out by the model to evaluate the effects of such parameters as input power, sample aspect ratio, and porosity on the rate of process. The results showed that higher input powers and sample volumes, as well as the use of bigger susceptors made the reaction enhanced. It was also shown that a decrease in the porosity and aspect ratio of sample leads to the enhancement of the process.

**Keywords:** Combustion Synthesis, Microwave Processing, Aluminum-Titanium Intermetallic Compounds, TiAl/Al<sub>2</sub>O<sub>3</sub> Composite, Numerical Modeling.

## 1. INTRODUCTION

Microwaves are used for many industrial and scientific purposes. Microwave use is a novel way of processing materials due to its special characteristics as a heating source; including its environment friendliness, reduction in time and energy consumption and also its ability to produce unique microstructures[1-3].

One of the microwave applications in material processing, which has a great potential for different innovations, is material synthesis[4-6]. Synthesis of ceramics and ceramic based materials is one of the great successes achieved[7]. Taking this achievement into account; its use as a new way of in-situ combustion synthesis of Intermetallics and their composites seems to be a great ground of study[8,10].

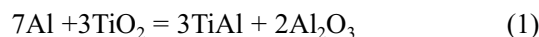
Numerical simulation of microwave processing has been the subject of various studies[11-20]. Alpert and Jerby numerically modeled the coupled thermal-electromagnetic heating of microwave [19]. Ying and others worked on numerical modeling of organic reactions [20]. However, numerical simulation of combustion synthesis of TiAl/Al<sub>2</sub>O<sub>3</sub> composite via microwave heating from the initial powder

mixture of TiO<sub>2</sub>/Al has not been numerically simulated till now.

In this study a numerical model has been developed to simulate the combustion synthesis of TiAl/ Al<sub>2</sub>O<sub>3</sub> composite via microwave heating. To verify the model, predicted results were compared with the data published in the literature. The model was further used to study the effect of different parameters on the combustion synthesis of TiAl/Al<sub>2</sub>O<sub>3</sub> composite.

## 2. NUMERICAL MODEL

A numerical model for microwave heating of a cylindrical compact of 3TiO<sub>2</sub>+7Al mixture of 8mm diameter and 4mm height was developed. It was assumed that two SiC blocks were placed on the two sides of the compact to absorb microwaves and convert their energy to heat. The combustion synthesis reaction was considered as follows:



The microwave input power was assumed to be 800 W and the oven was a single mode one.

## 2. 1. Governing Equations

A two-dimensional transient heat transfer equation in an axisymmetric plane enclosed to simulate the heat flow in the compact as follows:

$$\rho C_p \frac{\partial T}{\partial t} = \frac{\partial}{\partial z} \left( k \frac{\partial T}{\partial z} \right) + \frac{1}{r} \frac{\partial}{\partial r} \left( rk \frac{\partial T}{\partial r} \right) + S_{MIC} + S_{Melt} + S_{CS} \quad (2)$$

Where  $C_p$  is mixture specific heat at constant pressure ( $Jmol^{-1}K^{-1}$ ),  $\rho$  is mixture mass density ( $kg/m^3$ ) and  $k$  is mixture thermal conductivity ( $Wm^{-1}K^{-1}$ ).

$S_{MIC}$  is the microwave heating source term which was calculated from Maxwell equations, which are as follows:

$$\nabla \cdot \bar{D} = \bar{\rho}_e \quad (3)$$

$$(\nabla \times \bar{E}) + \frac{\partial \bar{B}}{\partial t} = 0 \quad (4)$$

$$\nabla \cdot \bar{B} = 0 \quad (5)$$

$$(\nabla \times \bar{H}) - \frac{\partial \bar{D}}{\partial t} = \bar{J} \quad (6)$$

Where  $E$  and  $H$  are electric and magnetic fields,  $D$  and  $B$  are electric displacement and magnetic induction,  $J$  is electric current density and  $\rho_e$  is volumetric electric charge density.

Assuming a single mode microwave applicator with TEM mode, the microwave heating source term was obtained as:

$$S_{MIC} = P_{ave} = \frac{\sigma(E_0)^2 \exp(-2\alpha d)}{2} \quad (7)$$

Where  $P_{ave}$  is the average power absorbed by the material ( $W/m^2$ ).  $\sigma$  is the specific electric conductivity ( $\Omega^{-1}m^{-2}$ ),  $E_0$  is the nominal electric field of microwave,  $d(m)$  is the distance between the point on the sample surface, where microwaves hit the sample, and a certain point inside the material.  $\alpha$  is defined as:

$$S_{Melt} = -\Delta H_{Melt} (\rho_i f_i - \rho_i^o f_i^o) \quad (8)$$

Where  $\mu_o$  is magnetic permeability of free space and  $\epsilon$  is electrical permittivity [21].

The second source term in equation (2) takes the melting of aluminium into account which is expressed as:

$$S_{Melt} = -\Delta H_{Melt} (\rho_i f_i - \rho_i^o f_i^o) \quad (9)$$

Where  $\Delta H_{Melt}$  is the enthalpy of melting of aluminum.  $\rho_i$  and  $\rho_i^o$  are the mass densities of mixture at the moment and at the previous step, respectively. Also,  $f_i$  and  $f_i^o$  are the volume fractions of molten aluminum at the moment and at the previous time step, respectively.

The last term in the energy equation (equation (2)) considers the heat evolved by exothermic reaction according to equation (10):

$$S_{CS} = \rho H \varphi (T, q) \quad (10)$$

Where  $H$  and  $\varphi (T, q)$  are the heat of reaction ( $kJ/mol$ ) and the rate of reaction ( $1/s$ ) respectively.

In order to calculate this source term, the rate of reaction ( $\varphi$ ) has to be known in priori. The following equation calculates the rate of fraction which is coupled with energy equation.

$$\varphi(T, q) = \frac{\partial q}{\partial t} = A(1, q) \exp\left(-\frac{E}{RT}\right) \quad (11)$$

In the above equation,  $q$  is reacted mole fraction,  $A$  is the pre-exponential constant,  $E$  is the activation energy ( $J/mol$ ) and  $R$  is the constant of gases.

## 2. 2. Initial and Boundary Conditions

The initial conditions for temperature were assumed to be 25 °C at any point, and the reacted fraction ( $q$ ) was assumed to be zero at initial time.

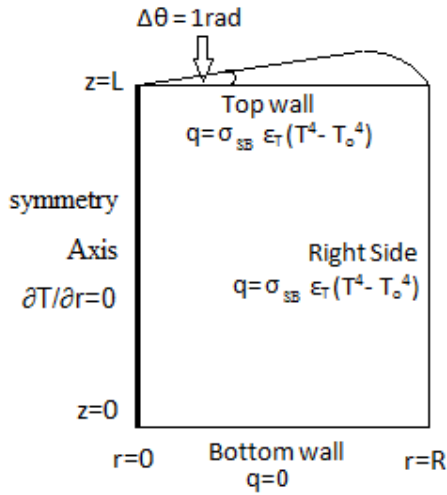


Fig. 1. The computational domain and associated boundary conditions used for the energy equation.

The boundary conditions for heat flow equation are shown in Figure 1, including radiation from the right and top walls (equation 12) and zero heating flux ( $q=0$ ) at the bottom wall and symmetry axis.

$$q = \sigma_{SB} \epsilon_T (T^4 - T_o^4) \quad (12)$$

In the above equation  $q$  is heat flux,  $\sigma_{SB}$  is Stefan-Boltzman constant;  $\epsilon_T$  is Emissivity factor and  $T_o$  is the ambient temperature to be set at 298K. Since the radiation is dominant, convective heat transfer is neglected.

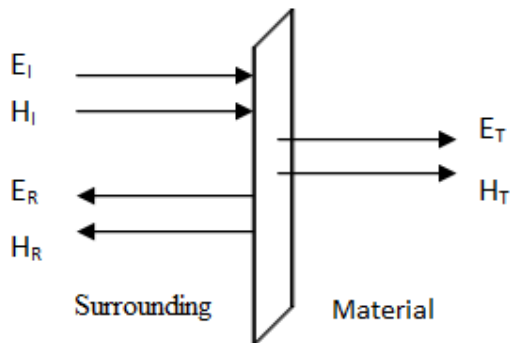


Fig. 2. Different waves at the material surface.

For microwave heating source term a set of boundary conditions is needed due to the differences between the materials and the surroundings. This situation is shown in figure 2; where,  $E_I$  and  $H_I$  are the incident,  $E_T$  and  $H_T$  are the transmitted and  $E_R$  and  $H_R$  are the reflected wave electric and magnetic parts respectively.

Accordingly, the boundary conditions for microwave will be:

$$E_T = \tau E_I \quad (13)$$

$$\tau = \left( \frac{2\eta_2}{\eta_1 + \eta_2} \right) \quad (14)$$

$$\eta = \left[ \frac{i\omega\mu_0}{\sigma + i\omega\epsilon} \right] \quad (15)$$

Where  $\tau$  is transmission coefficient,  $\eta$  is intrinsic impedance,  $\omega$  is angular frequency. Indices 1 and 2 refer to the surrounding and the material, respectively [21].

### 2. 3. Solution Methodology

Maxwell equations were solved by assuming the microwave to be single mode and TEM (Transverse Electromagnetic Mode)[21].  $\varphi$  equation was solved by considering the combustion reaction to take place in 4 minutes[22].

The governing heat transfer equation was solved by a computer code developed in Fortran 6.0 using finite volume method. A fully-implicit scheme was adopted to discretize the transient term. A Three Diagonal Matrix Algorithm (TDMA) was used to solve the discretized equations in each time step iteratively. The following convergence criterion for temperature was adopted:

$$R_T = \sum |a_p T_p - \sum a_{nb} T_{nb} - b| < 10^{-5} \quad (16)$$

Figure 3 shows the flow chart of the computer code.

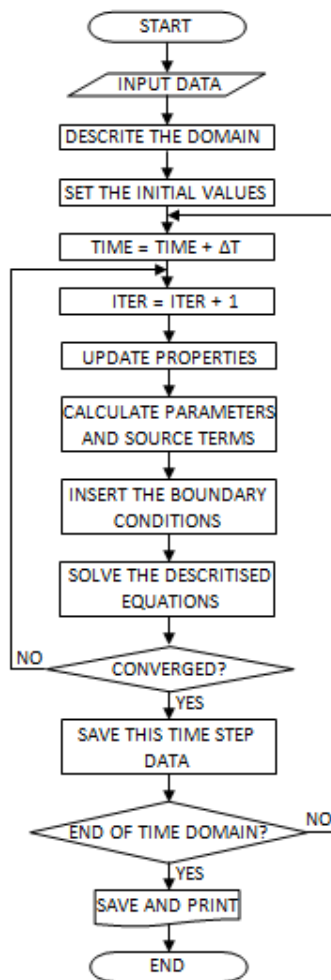


Fig. 3. Program flow chart.

### 3. RESULTS AND DISCUSSION

#### 3.1. Model Evaluation

The model was evaluated using the results obtained by Naplocha and Granat [22] where cylindrical plates of 23 mm diameter and 4mm height from compact Ti and Al powders were heated under microwave radiation of 240GHz in argon atmosphere and using a SiC block as susceptor. Figure 4 compares the temperature history of a certain point of the sample predicted by the present model with those measured by Naplocha and Granat. This point was considered to be on the radiating surface of the sample, on

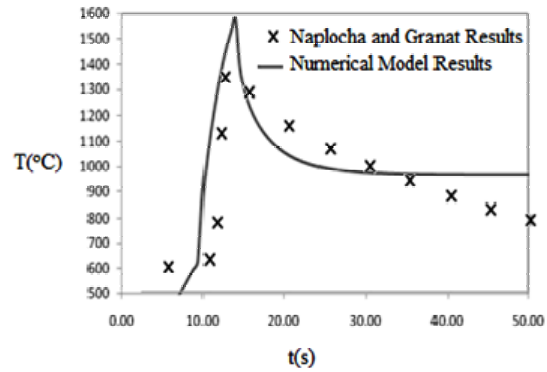


Fig. 4. Comparison of computed temperature history of a certain point with those measured by Naplocha [22].

the r-axis. Only a series of results has been shown here for the sake of brevity. A relatively good agreement has been achieved.

#### 3.2. Typical Computed Results

The typical results obtained from the model are for the sample with porosity of 25% which is located between two cylindrical SiC blocks with similar dimensions as the sample. In this case, the top surface of the sample is not radiative any more. Instead, the top surface of the upper SiC block becomes radiative and heat transfer from this block is similar to those for the block at the bottom. Figure 5 shows the variation of temperature along

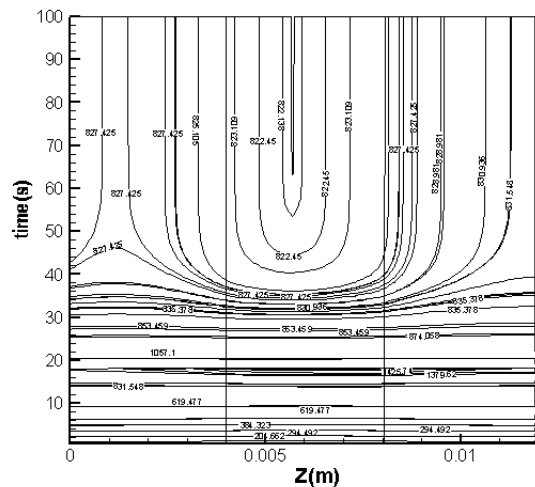


Fig. 5. Temperature Changes in z direction in central plate of sample at different times.

the z direction at the center of sample for different times. It is seen in figure 5 that the whole sample heats up fairly uniformly until the combustion synthesis begins. The uniformity is so that at any time, at different points in z direction the temperatures are the same or very close. This shows that the combustion synthesis has the explosion mode, so that the whole sample reaches up to the melting point at the same time and then combustion synthesis starts about the same time all over the sample.

Figure 6 represents the temperature history for a point located in the middle of the sample. From figure 6, it is seen that at a central point in the compact, the melting of Aluminum starts in about 10 seconds and after it finishes, the combustion synthesis starts and heats up the whole sample to temperatures about 1440 °C after the synthesis ends the temperature decreases. But because microwave heating by SiC still exists, temperature reaches 800 °C and then has no further changes. This can lead to an optimum microstructure due to maintenance at high temperatures, so that the product will be sintered effectively right after synthesis. Although, if this

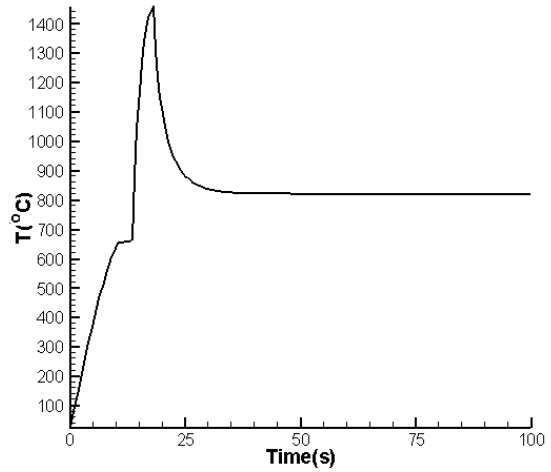


Fig. 6. Temperature History at a point at the center of powder compact.

is not desired, the microwave input power can be used to heat up the sample till the start of combustion synthesis and then stopped before 25 seconds which is the time of process completion.

Figure 7 shows temperature distribution in z

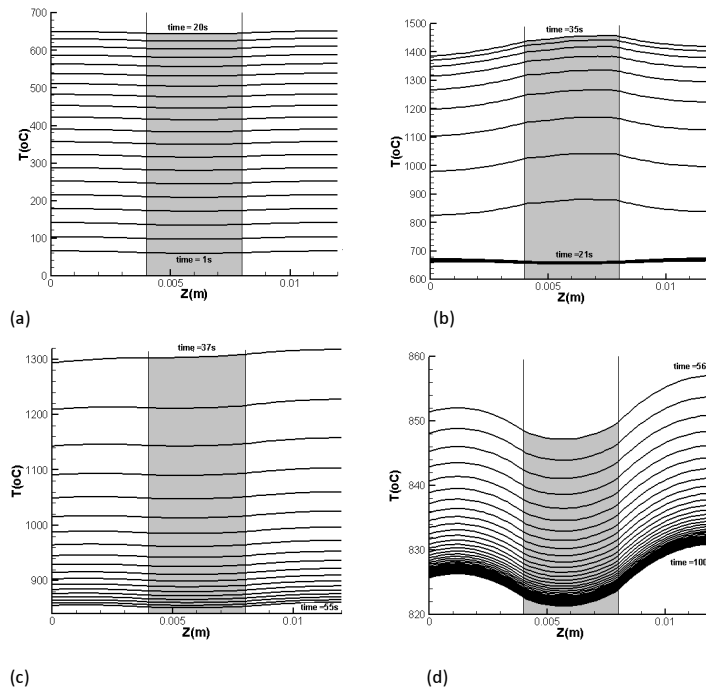


Figure 7. Temperature distribution in z direction: (a) at first 20 seconds, (b) from second 21 to 35, (c) from second 37 to 55, (d) from second 56 to 100, The gray area in each picture is the sample and the white ones are SiC blocks.

direction at different times. The left and right parts in the picture are SiC blocks and the central part is the powder compact. Temperature distribution in z direction is divided to four sections in Figure 7 to provide the possibility of further probation. As it is seen in part (a), at the first 20 seconds the whole sample heats up relatively uniformly till the melting temperature of Aluminum. The relatively uniform distribution of heat in the whole system is the result of the very high amount of heat generation by the SiC block for such a thin sample. In part (b) it is seen that because of melting, the temperature of sample is a little bit lower than the SiC blocks. Although, when the combustion synthesis begins the sample will become hotter than the blocks and reach temperatures about 1440 °C at second 35. After that, according to part (c) till the end of reaction, the temperature decreases and as in part (d) stays at amounts about 800 °C.

#### 4. PARAMETRIC STUDIES

##### 4. 1. Input Power

The effect of input power on maximum temperature is shown in figure 8. Figure 9 shows maximum temperature gradients between two points at the surface, one on the central line and the other on the edge obtained at different input powers after reaching the stability time. This parameter is a measure of heating uniformity. Figure 10 shows average heating rates till reaching stability time at different input powers. It can be seen from figures 8 to 10 that by increasing the

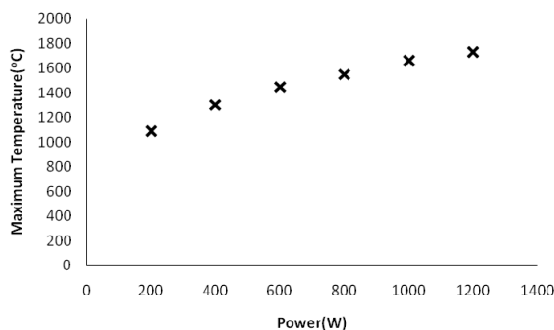


Fig. 8. Maximum temperatures at different input powers.

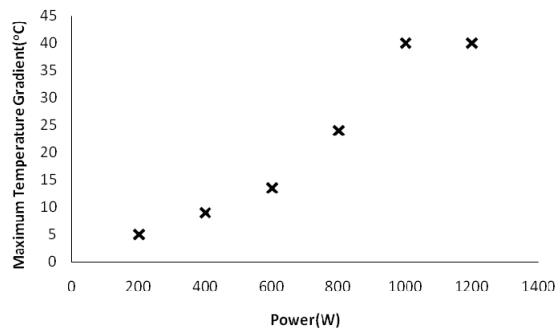


Fig. 9. Maximum temperature gradients at different input powers (one on the central line and the other on the edge after reaching the stability time).

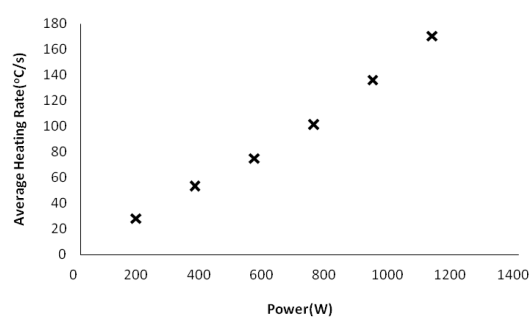


Fig. 10. Average heating rates at different input powers.

input power the maximum temperatures reached will be higher, but the increase is so that heating will become less uniform and temperature gradients will increase as well. Although the gradient will reach a constant value after reaching a certain input power. The heating rate also increases from 28 °C/second at 400 watts to 180 °C at 1200 Watts. This shows the important effect of input power on the heating rate.

##### 4. 2. Porosity

The effect of porosity on maximum temperature is shown in figure 11. Figure 12 shows maximum temperature gradients obtained at different porosity contents and figure 13 shows average heating rates till stability time at different porosity values. Porosity, as shown in figures 11 and 12, will have a negative effect on the temperatures obtained; but, will have a positive effect on heating uniformity. It might be due to a decrease in power concentration in certain positions inside the sample. Also it is shown that

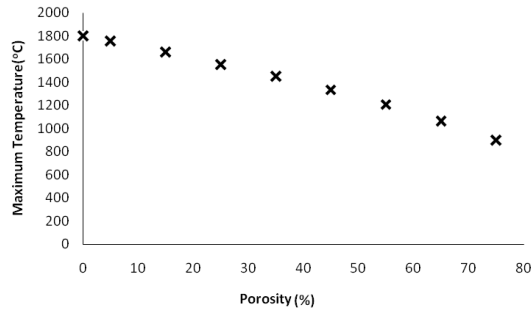


Fig. 11. Maximum temperatures at different porosity values.

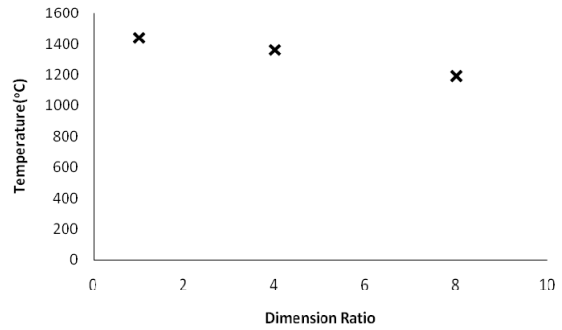


Fig. 14. Temperature at different dimension ratios.

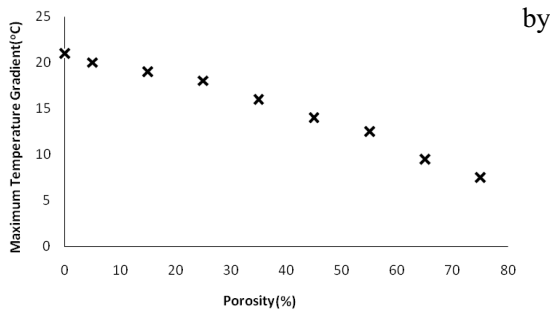


Fig. 12. Maximum temperature gradients at different porosity values.

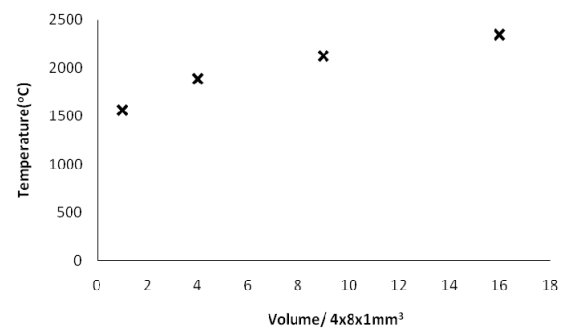


Fig. 15. Temperature at different volumes.

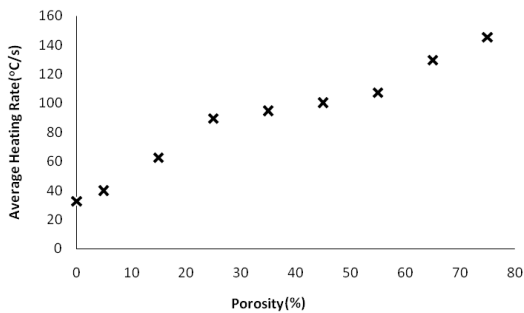


Fig. 13. Average heating rates at different porosity values.

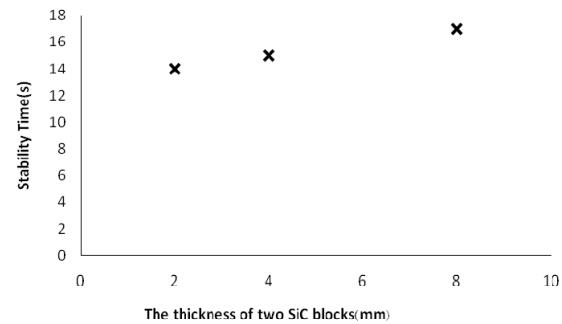


Fig. 16. Stability time at different SiC block sizes.

increasing the porosity, the heating rate will increase as well (Figure 13).

#### 4. 3. Aspect Ratio

Figure 14 shows the effect of different dimension ratios (diameter/height) on temperature and figure 15 shows the effect of

volume change on temperatures obtained. As seen in figures 14 and 15, by an increase in dimension ratio, the maximum temperature will decrease; and, by an increase in the sample volume, the temperature will increase.

Figure 16 and figure 17 show the effect of SiC block size on stability time (the time from which the temperature distribution profile won't change

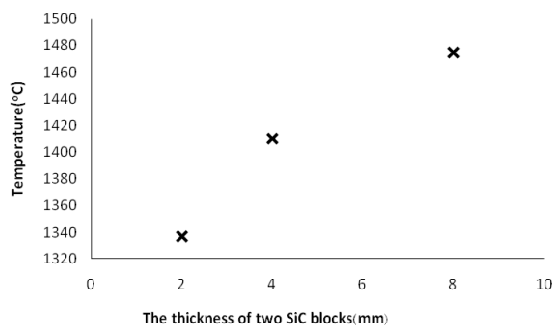


Fig. 17. Temperature at different SiC block sizes

with time passing by any more) and temperatures gained respectively. As shown in these figures, when the size of SiC blocks increases the stability time and the temperature will be higher.

## 5. CONCLUSIONS

1. In this study a numerical model for microwave heating  $\text{TiO}_2/\text{Al}$  powder mixture using two SiC blocks as microwave energy absorbers was developed.
2. The results showed highly uniform and volumetric heating of the mixture plate to the temperatures high enough for the combustion synthesis.
3. By an increase in input power, temperatures and heating rate increase, but the uniformity of heating decreases.
4. If the porosity increases, temperatures obtained decrease; but, the heating rate and heating uniformity increase.
5. It was shown that by an increase in aspect ratio, the temperatures decrease; but, if the volume of the sample increases, temperatures increase too.
6. If the thickness of SiC blocks increases, the stability time and obtained temperatures both increase.

## 6. ACKNOWLEDGMENT

The authors are grateful to the simulation group at Iran University of Science and Technology for their helpful comments.

## REFERENCES

1. Clark, D. E., Folz, D. C., West, J. K., "Processing Materials with Microwave Energy", *Materials Science and Engineering A287*: 153–158(2000).
2. Ku, H. S., Siores, E., Taube, A., Ball, J. A. R., "Productivity Improvement Through the Use of Industrial Microwave Technologies", *Computers & Industrial Engineering* 42: 281-290(2002).
3. Gupta, M., Wai Leong, W., "Microwaves and Metals", John Wiley and Sons (Asia) Pte. Ltd., 26-175(2007).
4. Zhou, G. T., Palchik, O., Pol, V. G., Sominski, E., Koltypin, Y., and Gedanken, A., "Microwave-assisted Solid-state Synthesis and Characterization of Intermetallic Compounds of  $\text{Li}_3\text{Bi}$  and  $\text{Li}_3\text{Sb}$ ", *Journal of Materials Chemistry*, 2607-2611(2003).
5. Xia, Q., Yi, J., Peng, Y., Luo, S., and Li, L., "Microwave Direct Synthesis of  $\text{MgB}_2$  Super Conductor" *Materials Letters*, Vol. 62, 4006-4008(2008).
6. Leske, J. W., Stagger, T. J., Aitken, J. A., "Microwave Metallurgy: Synthesis of Intermetallic Compounds via Microwave Irradiation", *Chemistry Materials*, Vol. 19, 3601-3603(2007).
7. Ahmad, I., "Unique Application of Microwave energy to the Processing of Ceramic Materials", *Journal of Microwave Power and Electromagnetic Energy*, Vol. 26, No. 3, 128-138(1991).
8. Gedevisishvili, S., Agrawal, D., Roy, R., "Microwave Combustion Synthesis and Sintering of Intermetallics and Alloys", *Journal of Materials Science Letters*, Vol. 18, 665-668(1999).
9. Poli, G., Sola, R., Veronesi, P., "Microwave-assisted Combustion Synthesis of NiAl Intermetallics in a Single Mode Applicator: Modeling and Optimization", *Materials Science and Engineering*, Vol. 441A, 149-157(2006).
10. Jokisaari, J. R., Bhaduri, S., Bhaduri, S. B., "Microwave Activated Combustion Synthesis of Titanium Aluminides",



- Materials Science and Engineering, Vol. 394A, 385-392(2005).
11. Jia, X., Jolly, P., "Simulation of Microwave Field and Power Distribution in a Cavity by a Three Dimensional Finite Element Method", *Journal of Microwave Power and Electromagnetic Energy*, Vol. 27, no1, 11-22(1992).
  12. Yee, K. S., "Numerical Solution of Initial Boundary Value Problems Involving Maxwell's Equations in Isotropic Media", *IEEE Transactions, Antennas Propagation*, Vol. 14, 302-307(1996).
  13. Pathak, V., Yun, Z., Iskander, M. F., "Development of an Integrated Multi-grid 3DFDTD and Finite-Difference Heat Transfer Code to Simulate Microwave Drying in Multimode Cavities", *IEEE*, 138-141(2001).
  14. Ma, L., Potheary, N. M., Railton, C. J., "Application of the FDTD Technique on Microwave Heating", *IEEE, Second International Conference on Computation in Electromagnetics*, 103-106(1994).
  15. White, M. J., Iskander, M. F., "A New FDTD Multi-Grid Technique with Dielectric-Transverse Capabilities", *IEEE 1997 Digest, Antennas and Propagation Society International Symposium*, Vol. 4, 2160 – 2163(1997).
  16. Shouzheng, Z., Davies, J. B., "Non Linear Modeling of Microwave Heating Problems", *IEEE, International Conference on Computation in Electromagnetics*, 86-89(1991).
  17. Chunshan, Y., Webin, F., Bihua, Z., "A Study on Perturbation Mode of Microwave Heating Substrate Temperature-Field", *IEEE, 3rd International Symposium on Electromagnetic Compatibility*, 672-674(2002).
  18. Pichon, L., Meyer, O., "Coupled Thermal-Electromagnetic Simulation of a Microwave Curing Cell", *IEEE Transactions on Magnetics*, Vol. 38, No.2, 977-980(2002).
  19. Alpert, Y., Jerby, E., "Coupled Thermal-Electromagnetic Model for Microwave Heating of Temperature-Dependent Dielectric Media", *IEEE Transactions on Plasma Science*, Vol. 27, No. 2, 555-562(1999).
  20. Ying, W., Youhaung, J., Aijun, W., Wenmiao, S., "Numerical Model of Microwave Heating to Organic Reaction", *IEEE ICCEA Proceeding*, 505-508(1999).
  21. Szekely, J., Evans, J. W., Brimacombe, J. K., "The Mathematical and Physical Modeling of Primary Metals Processing Operations", *John Wiley & Sons Inc., USA*, 662-688(1988).
  22. Naplocha, K., Granat, K., "Microwave Activated Combustion Synthesis of Porous Al-Ti structures for Composite Reinforcing", *Journal of Alloys and Compounds*, Vol. 486, 178-184(2009).